Received: 4 July 2023 | Revised: 22 August 2023 | Accepted: 25 August 2023

DOI: 10.1002/jcc.27224

SOFTWARE NOTE

Journal of COMPUTATIONAL CHEMISTRY WILEY

AOMadillo: A program for fitting angular overlap model parameters

Moritz Buchhorn | Vera Krewald

Theoretische Chemie, Technische Universität Darmstadt, Darmstadt, Germany

Correspondence
Vera Krewald, Theoretische Chemie, Technische Universität Darmstadt, Peter-Grünberg-Straße 4, 64287, Darmstadt, Germany.
Email: vera.krewald@tu-darmstadt.de

Funding information
Deutsche Forschungsgemeinschaft, Grant/Award Number: 443703006

Abstract

The angular overlap model (AOM) is an established parameterization scheme within ligand field theory (LFT). In principle, its application is fairly straightforward, but can be tedious and involve a trial-and-error approach to identify and judge the best set of parameters. With the availability of quantum chemical methods to predict d-d transitions in transition metal complexes, a rich source of computational spectroscopic data with unambiguous assignments to electronic states is available. Herein, we present AOMadillo, a software package that is designed to interface the output of *ab initio* LFT calculations from the ORCA suite of programs and performs a least-squares fit for a chosen AOM parameterization. Many steps of the AOM parameterization are automated, so that scans of geometric parameters and evaluations of sets of similar complexes are convenient. The fitting routine is highly configurable, allowing the efficient evaluation of different parameter sets.

KEYWORDS
angular overlap model, ligand field theory, quantum chemistry, transition metals

1 | INTRODUCTION

The angular overlap model (AOM) is a flavor of ligand field theory (LFT), which means it is concerned with the parameterization of d-d transitions in coordination complexes.[1,2] In contrast to other ligand field parameterizations, AOM parameters are local, that is, each ligand has its own set of parameters that describe the properties of this particular ligand in the complex. The promise of the AOM is thus to transfer the concept of functional groups to coordination chemistry.[3] AOM parameters are interpreted in terms of their sign and magnitude: positive parameters are considered to reflect a ligand to metal electron donating interaction, negative parameters an electron accepting interaction.[2,4] One property that comes with the concept of functional groups is the transferability of their parameters into different coordination complexes, a feature of the AOM that was sometimes assumed,[5,6] but also opposed on occasion.[7–9]

Every application of the AOM to a coordination compound requires the parameterization of the one-electron ligand field Hamiltonian V_{LF}, while the two-electron part is generally parameterized in terms of Racah or Condon–Shortley parameters.[2] A direct way for parameterizing V_{LF} is to express the energy of the electronic d states in terms of the chosen parameterization and to search for a best-fitting set of parameters that reproduce these states. An alternative, indirect approach is the treatment of each element in V_{LF} as an independent parameter, resulting in a maximum of 15 independent elements in a symmetric 5×5 matrix.[10] This corresponds to the Wybourne parameterization of a C_1 complex.[11] The two-electron part is again fitted with Racah or Condon–Shortley parameters. The application of the AOM takes place in a second step, where solely V_{LF} is fitted with a chosen set of AOM parameters. AOMadillo employs the second, indirect way by fitting the ligand field Hamiltonian.

Each matrix element is expressed in terms of the general AOM equation.[1,11,12]

$$v_{ij} = \delta_{ij}E + \sum_L \sum_\lambda F_{L,\lambda,i} F_{L,\lambda,j} e_{L,\lambda} + \sum_L F_{ds,i}\sqrt{e_{L,ds}} \cdot \sum_L F_{ds,j}\sqrt{e_{L,ds}}. \quad (1)$$

E is the spherical contribution to the field, $F_{L,\lambda,i}$ are the angular overlap factors where L specifies the ligand, λ indicates the interaction type which can be σ, π_x or π_y, and i,j are the matrix element indices. F is a function of the angular coordinates of the ligands θ,ϕ,ψ and tabulated.[2] The parameters e capture the bond length dependent part and are subject to the ligand field fitting procedure. e_{ds} is a parameter that accounts for the d–s orbital mixing in complexes of certain symmetries.[12,13] Considering e_{ds}, each ligand can thus be parameterized by two to four parameters (see also Section 4.1), which leaves 13 parameters for an average octahedral ($E+6\cdot e_\sigma+6\cdot e_\pi$) or square planar complex ($E+4\cdot e_\sigma+4\cdot e_\pi+4\cdot e_{ds}$). Given that V_{LF} has a *maximum* of 15 independent elements, it is apparent that the AOM equation system is very likely to be underdetermined.

An interesting dilemma arises at this step: in order to solve the equation system resulting from the AOM parameterization, it is advisable to reduce its complexity. If there are symmetry features in the molecule, these can be used to lower the number of unique elements in the ligand field matrix which makes it easier to calculate the overlap factors and reduces the load of equations. The downside is that almost inevitably an underdetermined equation system results, so that dependencies arise and an infinite number of solutions can be found. It is therefore necessary to reduce the number of AOM parameters and thereby make the equation system determined. Reducing the parameters can be achieved for instance by fixing the ratios of certain parameters or by setting some parameters to zero. However, these choices are driven by the experience and biases of the researcher. The resulting simplifications may underestimate or neglect parameters or overlook the uniqueness of ligands.

The researcher is thus faced with a difficult choice between two options: the introduction of perhaps biased experience into the AOM parameterization, or a much more complicated but often enough analytically unsolvable equation system with a more impartial and complete parameter fit. In the rest of this work, we present how the AOMadillo package mitigates this dilemma by making the evaluation of ligand field Hamiltonians for asymmetric molecules feasible. In many cases, more insightful parameter sets are obtained than with simplifications that may result in underdetermined equation systems.

Starting with version 4, the ORCA quantum chemistry package offers an *ab initio LFT* (aiLFT) module.[14,15] With the electronic states from a CASSCF calculation, the aiLFT module fits the one-electron ligand field matrix and the two-electron Racah and Slater–Condon parameters. The corresponding CASSCF (CASSCF/NEVPT2) states together with the aiLFT module were shown to reproduce experimental data very well on several occasions.[16–20] The most important feature of this theoretical approach to AOM parameters is that, in contrast to the experiment, the investigated structures are rigid. The resulting states are sensitive to the exact input structure instead of an average one. It is thus possible to intentionally make structures that are asymmetric and because the AOM F-factors are angle-dependent, they can account for the changes in the electronic state energies. With this, it is possible to reliably increase the number of independent elements in V_{LF}, so that more parameters can be fitted. More details on the asymmetric structures are provided in Section 3. All our results are based on ORCA CASSCF calculations which AOMadillo interfaces to perform the AOM parameter fit.

2 | FUNCTIONALITIES OF AOMADILLO

AOMadillo offers a fast and easy application of the AOM to a ligand field Hamiltonian. The quality of the parameterization can be evaluated via the cost of the fit, a semi-objective quantity further elaborated below. This allows a straightforward comparison of different parameterization choices. The input and output work in a stand-alone way, and are designed such that they can be embedded in a shell pipeline. This allows the user to write simple shell scripts to test different parameterizations, scan the parameter space, and process output parameters for further analyses or visualizations. With ORCA as the quantum chemistry software that generates the ligand field Hamiltonian, the user has access to many other means of scanning and automation. The scheme in Figure 1 shows the steps that are necessary to generate an AOM parameterization with AOMadillo.

AOMadillo interfaces the output of the ORCA aiLFT module. Both ORCA 4 and ORCA 5 are supported. It reads the one-electron ligand field Hamiltonian V_{LF} and applies a fitting procedure developed by us to obtain the AOM parameters.[21] In the rest of this section, we provide a more detailed description of the procedure.

Each Hamiltonian matrix element is expressed as in Equation (1). Each value v_{ij} is calculated by ORCA and thus a known quantity in our problem. It is brought to the right side of the equation, which should then equal 0.

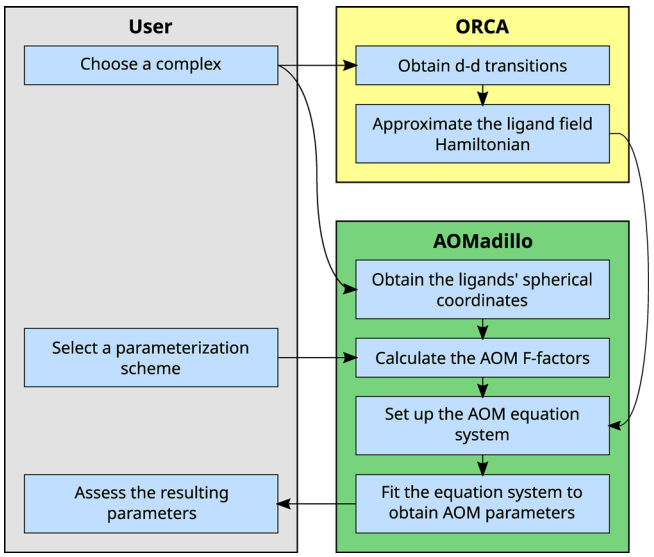

FIGURE 1 Schematic representation of the steps necessary to take full advantage of the AOMadillo package.

$$0 = -v_{ij} + \delta_{ij}E + \sum_L \sum_\lambda F_{L,\lambda,i} F_{L,\lambda,j} e_{L,\lambda} + \sum_L F_{ds,i}\sqrt{e_{L,ds}} \cdot \sum_L F_{ds,j}\sqrt{e_{L,ds}}. \quad (2)$$

Since the total equation system is in general overdetermined (see Section 3) and inconsistent, no set of parameters can be found that satisfies all equations. Instead, an approximate solution is found by employing a nonlinear least-squares solver and in the above equation 0 is replaced by the so-called residual s_{ij}.[22–24]

$$s_{ij} = -v_{ij} + \delta_{ij}E + \sum_L \sum_\lambda F_{L,\lambda,i} F_{L,\lambda,j} e_{L,\lambda} + \sum_L F_{ds,i}\sqrt{e_{L,ds}} \cdot \sum_L F_{ds,j}\sqrt{e_{L,ds}}. \quad (3)$$

The least-squares solver minimizes the equation system with regard to the sum of all equations squared residues s. We refer to this quantity as the "cost" of a fit and omit its dimension or unit, respectively, in the rest of this text.

$$cost = \sum_j \sum_{i \le j} s_{ij}^2. \quad (4)$$

V_{LF} is symmetric, so the cost is calculated from the elements s with $i \le j$ to prevent double counting. The cost can serve as a probe for the quality of a chosen parameterization. When choosing a parameter set that can reproduce the given ligand field Hamiltonian well, the cost is small. Otherwise the cost increases if we chose a set that poorly recovers the Hamiltonian. This assessment can only be applied in a relative manner, that is, if the parameterization is changed and the cost changes at the same time. The specific value of the cost of a single fit does not tell anything about its quality, although a high remaining cost in a detailed parameter set can be seen as a hint that the AOM in the given parameterization might be unsuitable.

Summarized briefly, the AOMadillo software offers the direct application of the AOM to aiLFT results. An obvious advantage over manually or semi-manually solving the AOM equations is that the computer delivers the result. Provided with only the molecular geometry, the program outputs the corresponding equation system, including the on-axis angle ψ which can be tedious to determine manually. A second advantage of AOMadillo lies in the configuration options for the parameterization and the ease with which restraints can be introduced. This allows a fast application of different parameter sets for comparison and batch processing of calculated transitions. In the next sections, the features of AOMadillo are presented in a qualitative overview. For detailed guidance on the actual utilization of the package, the reader is referred to the manual, which is provided with the software package.

2.1 | Possible parameterizations

The AOMadillo package offers various options for parameterization of the ligand field. The default is a parameterization with e_σ, e_π, e_{ds} for each ligand, where d–s mixing is considered and the two π-interactions are subsumed.

The d–s mixing parameter can be removed with a flag. This is advisable when the molecule is sufficiently close to a cubic symmetry (O_h or T_d), where d–s mixing plays no role.[4,10,12]

Similarly, the π-interaction can be removed, although we do not recommend this at all. Even for ligands that had been considered σ-only so far, we expect a significant π-interaction.[25]

The two π-interactions e_{π_x} and e_{π_y} can be discerned, which increases the parameter space. The additional angle that needs to be defined can be either provided by the user or calculated from the structure of the molecule. In the latter case, a third atom number is specified that defines a plane containing M–L–R which is perpendicular to the π_y-interaction. Vice versa, the π_x-interaction is then defined to lie in the M–L–R plane. Some publications denote the e_{π_x} and e_{π_y} parameters with $e_{\pi\parallel}$ and $e_{\pi\perp}$ to clarify their alignment relative to the respective ligand.[4,26]

2.2 | Parameter restraints

In addition to global changes of the parameterization scheme, restraints can be introduced. In AOMadillo, hard and soft restraints are distinguished depending on how they are implemented. Hard restraints are those that cannot be violated, no matter how it may increase the cost of the fit. Examples of hard restraints are removing parameters as mentioned above, or setting fixed values for individual parameters. These values cannot be changed during the fitting routine, but are taken into account when calculating the cost.

Soft restraints are introduced as additional equations to the fitting procedure. If the fit deviates from the value specified in the additional equations, the overall cost increases. This permits the parameters to take values that differ from the given restraint. It is of course possible to set soft requirements that cause high costs when they are slightly violated, making them effectively hard.

Natively supported soft restraints are equal e_λ parameters for different ligands and equal π_x, π_y interactions for selected ligands. Setting AOM parameters to be equal via a soft restraint is termed "grouping" in AOMadillo. Additional arbitrary restraints can be introduced by providing equations directly, for example to set a value, a ratio or a difference for selected parameters.

An important role of soft restraints is the introduction of independent equations to the system. Given that common complexes with six ligands and three parameters per ligand already exceed the maximum possible number of independent elements in V_{LF}, it is common to group ligands. We intentionally chose the addition of equations over the reduction of the number of parameters to account for small inequalities in the ligands positions and chemical environments.

3 | LIFTING THE UNDERDETERMINATION PROBLEM

Even when the number of AOM parameters is cleverly reduced, the equation system for many complexes remains underdetermined.

TABLE 1 Exemplary bond angles in degrees from a set of samples of $[CrCl_6]^{3-}$.

Sample	Cl1–Cr–Cl2	Cl3–Cr–Cl4	Cl5–Cr–Cl6	Cl1–Cr–Cl3	Cl1–Cr–Cl5
0	180.000	180.000	180.000	90.000	90.027
1	179.059	179.317	179.243	90.752	89.502
2	179.916	179.262	178.913	89.315	89.368
3	179.403	178.897	179.111	89.969	90.164
4	179.044	179.287	179.226	90.158	89.401
5	179.834	179.363	179.029	89.330	89.804

Note: The atoms 1, 2 and 3, 4 and 5, 6 are situated *trans* to each other. Sample 0 is the reference structure.

The higher the symmetry of the complex, the fewer unique elements V_{LF} has.[11] In an experiment, the observed transitions always belong to an ensemble of distorted structures, yielding broadened peaks. The underlying transitions cannot be completely resolved and thus it is necessary to assign the peaks to an assumed average geometry with generally high symmetry. Furthermore, many d-d transitions are hard to detect since they are generally weak and sometimes hidden under other, overlapping transitions. While computational spectroscopy has its own shortcomings, employing computational methods to calculate electronic transitions allows to overcome a few of these problems. Some of these advantages are that there is no ambiguity in the computed spectrum regarding the resolution and the assignment of a transition.

The key to lifting the underdetermination problem lies in intentionally creating asymmetric structures. Here, we make use of the transferability promise of the AOM that works in very limited cases, that is, the same ligand will have comparable AOM parameters in similar bonding situations. If AOMadillo is used with a high-symmetry structure, the ligands are moved slightly in random directions.* Asymmetric structures that yield ligand field potentials with a sufficient number of unique elements are obtained by starting from an optimized geometry. The bond angles are slightly changed while keeping the metal-ligand distance constant. In general, this leads to C_1 symmetry, in which 15 unique matrix elements are available for fitting. The result should be as asymmetric as possible while still being sufficiently similar to the reference structure to justify the AOM parameters to be equal. An example with distorted bond angles is shown in Table 1. We have shown previously that this approach works and allows to fit AOM parameters to formerly underdetermined problems such as tetrahedral[21] and octahedral[25] complexes.

Since the structural distortion uses small random angles of $\leq 0.5^\circ$, two issues can arise. First, the distortion can be too small so that the resulting equation system is still (partly) underdetermined. Second, the resulting structure might be biased: bond angles differ from the average, the ligands might be shifted to one side and so forth. While this does not necessarily pose a problem for the CASSCF calculation and the subsequent fit, we noticed that some structures yield parameter sets that clearly differ from others. We cannot find a common explanation for these observed outliers, and suspect from our broad experience with different transition metals, coordination environments and ligand types that this effect is highly dependent on the chemistry of the system. Outliers should be identifiable among a sufficiently large number of samples. We recommend performing the structural distortion several times and separately fitting parameters for each distorted structure. In this way, outliers can be identified more easily and the danger of having a non-representative parameter set is reduced.

4 | THE USER'S TASKS

4.1 | Choosing a parameter set

Choosing the parameter set is crucial and may require several attempts in order to recognize bad fitting results, underdetermination problems and specific ligand behaviors. This is an important task that must be conducted carefully by the user. The following points may serve as a guide to evaluate which parameters are sensible to use.

Check for equal ligands: The first step is to check the ligand symmetries and similarities. It is useful to group equal ligands together, although differences in bond length are very important to consider here. Since the AOM parameters are bond length dependent, grouping different bond lengths can lead to conflicting equations that prevent a reasonable solution of the AOM equation system. Nonetheless, grouping bonds of up to approximately 0.1 Å difference can work occasionally. When deciding on the acceptable bond length difference for grouping, the user needs to consider the slope of the distance dependence; while for transition metals the distance dependence of Δ is expected to be r^{-5},[27,28] for lanthanides and actinides it is much steeper, ca. r^{-7}.[27]

Assess bond symmetry: The next step is to check whether the individual metal-ligand bonds are cylindrical, that is, have $C_{\infty v}$ symmetry. This is not an automated process but rather a step where the users can take important decisions on the parameterization themselves. For symmetric bonds, e_{π_x} and e_{π_y} can be subsumed. If the bond is asymmetric, they must be distinguished. Examples for ligands with cylindrical bonds are halides, NH_3, CO, CN^-, metallocenes and others. Asymmetric bonds are found for example with water, pyridine and other heterocyclic ligands.

Assess global symmetry: The global symmetry of the coordination site should be evaluated. This is not done automatically by AOMadillo, but programs that can determine the closest global

symmetry automatically are available if assistance is required. If at least one d orbital transforms in the totally symmetric irreducible representation of the point group of the coordination site, one must consider d–s mixing.

Based on the parameterization chosen by the user, AOMadillo can be configured to perform the fit accordingly. Note that a chemically plausible set of parameters does not necessarily lead to a good fitting result. A good result is considered to be (over-)determined, low-cost and with parameters of a reasonable magnitude.

4.2 | Assessing the result

The equation systems generally converge well. We never encountered a system where convergence was not achievable, although convergence of a mathematical solution to the equation system is not to be confused with obtaining reasonable parameter values. It is still possible that the system is underdetermined, in which case convergence will be signaled but the resulting fit is not unique. Note that the equation system can be partly underdetermined (see, for example, Section 7.3). In these cases, some of the parameters are reliable to a certain extent, while others depend on each other and are not unique. Because of this, a cost larger than zero does not guarantee an overdetermined system. We recommend to scan the parameter space around the solution in order to recognize partial underdetermination situations.

The cost of a fit is an important quantity to check. High cost values (>1000 cm^{-2}) are most often caused by an incomplete parameterization, inappropriate ligand grouping or other hard to meet soft restraints. If tweaking groupings and parameter sets does not improve the cost, a suitable parameterization might not be attainable, see Section 5.1.

The resulting parameters should be of reasonable magnitude, that is, within the expectations set by the literature or previous parameterizations of similar systems. An obvious case of an unreliable result is for example a negative e_σ parameter. Parameters with significant differences for almost equal ligands or parameters that deviate strongly from reported data are also signs of error.

5 | LIMITATIONS

LFT, ORCA aiLFT and AOMadillo have important limitations that the user needs to be aware of. Some problems rooted in the general theory are carried over to the AOM parameterization. In the following, we will discuss how apparently nonsensical results can be interpreted, what to check before the fit is done and when LFT as such may fail.

Ligand field theory and ORCA aiLFT

LFT assumes pure valence d orbitals, which is a good assumption if there is essentially no mixing or covalency between metals and ligands. This can be the case if the ligand orbitals are much lower in energy than the metal orbitals. The observed "pure" d orbitals are then in fact the antibonding metal-ligand molecular orbitals. In electronic structure calculations, it is readily seen that the valence molecular orbitals are composed of metal and ligand contributions of different magnitude. LFT is essentially an effective Hamiltonian theory,[4,29] and as such it is more successful if the configurational space described by the effective Hamiltonian (here the complete ligand field Hamiltonian) is well separated from the rest of the basis.[10,30] With a decrease of the d orbital contribution to the MOs, that is, more covalent bonds, LFT increasingly looses its justification and obtained parameterizations should be interpreted with caution.

ORCA purifies the metal d orbitals when the aiLFT subroutine is called in order to obtain an active space that fits to the assumptions of LFT.[31,32] Nonetheless, the resulting orbitals can still have significant ligand character. Especially for more covalently bound ligands like CN^- or PMe_3, d orbital contributions of about 80% and less to an active orbital are common. For ligands like halides, we generally find orbitals with more than 90% d character. Note that this can make it difficult to describe some common ligands with π-backbonding capabilities, since they arise from metal and ligand AOs that are close in energy and thus strongly mix.

Lastly, if LFT can be applied to a complex and a reasonable parameterization can be made, the calculation itself can have systematic errors. The states predicted by CASSCF or CASSCF/NEVPT2 calculations are associated with errors arising, for example, from the active space size, the basis set size, or the treatment of the environment. These errors translate into the ligand field Hamiltonian. In consequence, the user needs to set up the ORCA calculation according to the desired accuracy and inclusion of environment effects.

AOMadillo

AOMadillo applies the AOM equations to the aiLFT output of ORCA and returns a fitted set of parameters; however it does not provide any further comment on the set. Depending on the complex at hand, the least-squares fitting procedure can have multiple results with the same cost for different parameterizations. While it is possible to scan the parameter space around the solution obtained to find out how deep or well-defined the minimum is, this information does not tell the user how chemically reasonable the solution is. Judging the parameter set is thus a task obliged to the user.

It can be helpful to have a closer look at the AOM parameters of different structure samples. With sample set sizes of five as commonly employed in our initial studies, it has been observed that some samples yield unreasonable results. A unique reason for the outliers has not been identified, but the user is encouraged to investigate the structures further if fits with diverging results are obtained. Additional aiLFT calculations with more samples, possibly including a slight variation of bond lengths in addition to different angles, can be useful to deduce which results are actual outliers.

5.1 | Advanced aspects of the AOM

There are extensions of the AOM that are not yet supported by AOMadillo. One example is d–p mixing,[33] where in principle the same sequence of arguments as for d–s mixing applies. Very often, d–p mixing is subsumed with other parameters and cannot be separated. There are special cases where it becomes relevant and needs parameterization on its own, as for example encountered in Section 7.2. Since the chemical significance of the AOM may suffer by introducing more global parameters, we decided not to implement it.

Another extension is the Orgel effect or phase-coupled ligation.[34–38] Different treatments and discussions exist in the literature. At the moment no variant is implemented in AOMadillo, which precludes fitting systems with chelating ligands that have conjugated π-systems properly.

Similarly, misdirected valency or off-axis bonding is currently not implemented. Misdirected valency occurs when no symmetry axis of the ligand coincides with the metal-ligand bond. More pictorially speaking, in cases where misdirected valency is important, the ligand does not point exactly at the metal which leads to an orbital energy splitting that cannot be accounted for in terms of distinct σ or π parameters. It is possible to parameterize the resulting splitting with additional AOM parameters which are placed in the off-diagonals of the ligands' local ligand-field matrices.[30,38–42] These additional parameters may have less obvious chemical significance and rather represent a means to describe a geometric peculiarity within the AOM framework.

5.2 | Metals with f shells

The AOM is generally suitable to parameterize elements with partially filled f orbitals.[43,44] Urland and coworkers have worked on this topic extensively, including the derivation of the corresponding overlap factors for these elements.[11,45] The aiLFT module of ORCA provides an f orbital analysis, yielding a 7×7 ligand field matrix V_{LF}. In AOMadillo, the analysis of these aiLFT calculations is not yet implemented.

5.3 | Inclusion of δ interactions

It is common practise in the application of the AOM to omit e_δ entirely.[7] It is considered small and often leads to overparameterization without additional chemical insight. We therefore decided not to implement it into the fitting routine.

6 | DETAILS

This section provides background information on how certain functions are derived and implemented. For more details on the practical application of the AOMadillo program, we refer the reader to the manual, where a detailed walkthrough is provided.

6.1 | Structure sampling

Structural sampling is crucial to lift the underdetermination problem of the AOM parameterization. It is also important to calculate parameters for several samples, since there might be outliers that can only be recognized in comparison to other parameter sets. In the AOMadillo package, the structural distortions are performed by a dedicated script; the manual provides details on its application. The sampling procedure takes Cartesian coordinates and a definition of ligands as input. Each ligand is then independently rotated by three random Euler angles in a given interval. The interval we use is $[0.2, 0.5]$, which has proven sufficient to yield completely asymmetric structures with sufficiently large energy differences in the ORCA aiLFT Hamiltonian. It is possible to apply the procedure to chelating and $\eta^{(>1)}$ ligands, too. Depending on the ligand structure, a dummy atom in the center of the ligand may need to be defined which is then used as an anchor. For example, cyclopentadienyl (Cp^-) needs a dummy atom in the center of the ring, and ethylenediamine (en) can be moved with a dummy atom between the nitrogen or the carbon atoms.

When the samples are created, it is possible to read in orbitals from another CASSCF calculation performed on the original structure. ORCA has an orbital projection feature that can translate these orbitals onto the sample structures, hence one converged CASSCF calculation can be used as input for the subsequent samples, speeding up the process significantly.

Another feature embedded in the sampling procedure is the option to perform bond length scans. An interval with minimum and maximum bond length as well as the number of steps can be defined. The ligands are then moved accordingly. Note that although possible with the help of dummy atoms, this is not useful for chelating ligands, since their L–M–L bond angles are changed by this as well.

6.2 | AOM equation system

The one electron ligand field matrix is a 5×5 symmetric matrix, so it has up to 15 unique elements. Each element is expressed in terms of Equation (3), with v_{ij} being calculated by ORCA and the AOM overlap factors calculated from the structure of the complex. In general, this equation system is inconsistent and overdetermined. That means there is no set of parameters that satisfies all equations and there are more equations than parameters. Since there is no exact solution, an approximate one is found with the least-squares approximation mentioned in Section 2.

The parameters have hard coded boundaries: all local AOM parameters can have values in the interval $e_\lambda/\mathrm{cm}^{-1} \in [-2 \times 10^5, 2 \times 10^5]$, $e_{ds}/\mathrm{cm}^{-1} \in [0, 10^4]$ and $E/\mathrm{cm}^{-1} \in [-10^7, 0]$.

Soft restraints add equations to the base system. Grouping ligands adds equations of the following structure:

$$s_i = (e_{\lambda,L1} - e_{\lambda,L2}) \cdot w, \tag{5}$$

with $L1$ and $L2$ being arbitrary ligands and λ being the interaction type. The weighting factor w can be adjusted to increase or decrease the

effect of the restraint on the solution. s is the residue of the equation, its index i is a running number. In the same manner the equality of π_x and π_y-interactions can be set:

$$s_i = (e_{\pi_x,L} - e_{\pi_y,L}) \cdot w. \tag{6}$$

The least-squares solver will minimize the total cost and thus the absolute residues, so the requirements are met if the parameters are equal and their difference is zero.

With these additional equations, it is possible to have enough linearly independent equations to fit a large set of parameters. As stated, it has proven to be more effective if equations are added compared to the reduction of parameters. The possibility that a restraint can be violated adds valuable flexibility to the fit.

It is possible to add arbitrary equations to the system by giving expressions that should evaluate to zero. Only the right-hand side of the following equations must be given. This can be used to set parameter values without actually enforcing them or introduce ratios and differences. Here are some examples:

$$s_i = e_{\sigma,L} - 6000, \tag{7}$$

$$s_i = 4e_{\pi,L} - e_{\sigma,L}, \tag{8}$$

$$s_i = e_{\pi_y} - e_{\pi_x} - 1000. \tag{9}$$

It is up to the user to employ supplemental equations. They are provided to AOMadillo in an optional file; the standard configuration is not to expect such a file. We also note that introducing restraints removes impartiality from the result and should be well justified.

6.3 | Definition of π_x and π_y

It is chemically intuitive that planar ligands like water or pyridine have different π interactions in- and out-of-plane. To distinguish π_x and π_y, we have to resort to the definition of the parameters in the local parameter frame, where the ligand atom resides on the z-axis. The ligand field matrix expressed in the local d orbital basis for each ligand is:

$$V_{LF,local} = \begin{array}{c} \\ xy \\ yz \\ z^2 \\ xz \\ x^2-y^2 \end{array} \begin{array}{c} \begin{array}{ccccc} xy & yz & z^2 & xz & x^2-y^2 \end{array} \\ \begin{pmatrix} e_\delta & & & & 0 \\ & e_{\pi_y} & & & \\ & & e_\sigma & & \\ & & & e_{\pi_x} & \\ 0 & & & & e_\delta \end{pmatrix} \end{array}, \tag{10}$$

where e_δ is generally assumed to be 0. The superposition principle of the AOM requires to set up this matrix for each ligand, rotate it from its local to the global axis frame and then add it to the total ligand field matrix.[4,45] This rotation of the local basis can be expressed in terms of Wigner rotation matrices, which represent rotations of spherical harmonics along the three Euler angles θ,ϕ,ψ.[11,13] The Euler angles are equivalent to the global angular coordinates of the respective ligand, since it is the ligands' global position from which the d orbital basis must be rotated. The sequence of the rotations is fixed such that the ones along θ and ϕ have to be applied in that sequence, while the rotation along ψ can be applied any time.[11,46]

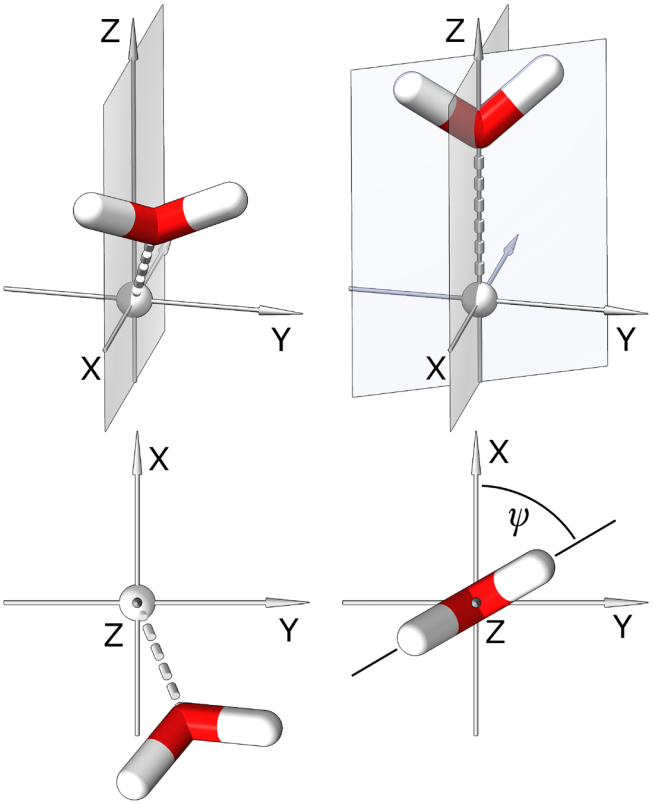

FIGURE 2 Illustration of the rotation of a ligand from an arbitrary position (left, top and bottom) onto the z-axis (right, top and bottom). The remaining angle between the ligand plane and the xz-plane is the angle ψ. The left and right frames each show the same situation from different perspectives in the top and bottom panels.

Employing that rule, we determine ψ for each ligand by rotating it back into its local frame. The ligand is thus rotated by $-\phi$ along the global z-axis and $-\theta$ along the global y-axis. An illustration of this rotation is shown in Figure 2. Additional to the metal position and the ligating atom, an orientation atom is specified that defines the ligand plane, for example, a hydrogen atom in water. The angle between the xz plane and the ligand plane is then ψ, as shown in the bottom right frame in Figure 2. If it is 0, the ligand plane coincides with the xz plane. By this definition, the parameter e_{π_x} lies in the ligand plane, while e_{π_y} is perpendicular, as stated in Section 2.1.

When applying the AOMadillo fitting routine with distinct π_x and π_y interactions, it is possible to specify ψ manually for each ligand, or to specify an orientation atom that, together with the metal and the ligating atom, defines the ligand plane.

7 | CASE STUDIES

7.1 | Methodology

All quantum chemical calculations were performed using the ORCA 4.2.1 software package.[14,15] The geometries of the $[Mn(NH_3)_n]^{2+}$ series were constructed from scratch. The structure of $Cu(NH_3)_4(SCN)_2$ was extracted from the crystal structure[47] with a subsequent optimization of the hydrogen atom positions. The structures of the platinum complexes and the ferric thiocyanates were fully optimized. Optimizations employed the unrestricted Kohn–Sham formalism with the BP86 functional,[48,49] the def2-SVP basis set[50] with the def2/J auxiliary basis.[51] The resolution of identity approximation for the Coulomb term was used.[52,53] Convergence criteria were NormalSCF for all self-consistent field calculations and TightOpt for geometry optimizations. The geometry optimizations employed the default integration grid (Accuracy 2: Lebedev 110 points) for optimization steps and the final SCF at the optimized geometry (Accuracy 4: Lebedev 302 points).

The electronic states corresponding to the d orbitals were calculated using CASSCF[54,55] with the def2-TZVP basis set.[50] For the platinum complexes, relativistic effects were captured with the zeroth order regular approximation (ZORA)[56] with the SARC-ZORA-def2-TZVP basis set for Pt and ZORA-def2-TZVP for other elements.[57] A CAS$(n,5)$ active space was chosen, containing n d electrons in the five valence d orbitals. The subsequent *ab initio* LFT analysis was used to construct the effective ligand field Hamiltonian.[10,18,44] AOM parameters were fitted with the software presented herein, AOMadillo. For each (optimized) complex, five distorted samples were generated.

7.2 | Ligand addition

The AOM promises at least a limited transferability of ligand parameters between different complexes. While it is well known that this is rarely reliable, AOMadillo allows the user to systematically check in which cases a transfer might be justified and in which not. In the next section, we discuss the mixing of ligand types in a heteroleptic complex. Here, a simpler case is investigated, where we focus on a series of complexes of the type $[Mn(NH_3)_n]^{2+}$, with $n = 1-6$. Each complex has the highest possible symmetry, which should be reasonable for manganese in the oxidation state +II due to its preferred high-spin d^5 electronic structure. In the case of $n = 5$, we investigated the trigonal bipyramidal case as well as the quadratic pyramidal one. All bond lengths were arbitrarily set to 2.1 Å and do not differ between coordination numbers to preserve comparability.

Table 2 and Figure 3 show the AOM parameters of the complexes. It is apparent that the magnitude of the parameters is the same for all complexes except the trigonal bipyramidal $n = 5$ case. The linear $n = 2$ complex also has a slightly deviating σ parameter, although this is due to a d–s mixing effect. Introducing d–s mixing here leads to a linear dependency of e_σ and e_{ds}; this effect is discussed in more detail in the next section on PtA_2B_2 complexes. Omitting a d–s mixing parameter leads the e_σ of the ligands to absorb its effect and decrease accordingly. If a fixed d–s mixing parameter of 715 cm^{-1} is introduced, we obtain $e_\sigma = 5375\ cm^{-1}$ which would fit perfectly to the other parameters in the series.

TABLE 2 AOM parameters of ammonia in $[Mn(NH_3)_n]^{2+}$.

n	Symmetry	e_σ/cm^{-1}	e_π/cm^{-1}	e_{ds}/cm^{-1}
1	lin.	5094 (0)	1557 (0)	
2	lin.	3945 (0)	1401 (0)	*a*
3	trig.	5780 (1)	1594 (151)	715 (101)
4	tet.	5726 (168)	1588 (125)	
5	trig. bipy.	10700 (229)	4486 (179)	*b*
5	quad. py.	7097 (39)	1713 (42)	2524 (92)
6	oct.	5813 (56)	781 (42)	

Note: *a* not included, but relevant; see main text for details. *b* subject to d–p mixing; see main text for details.

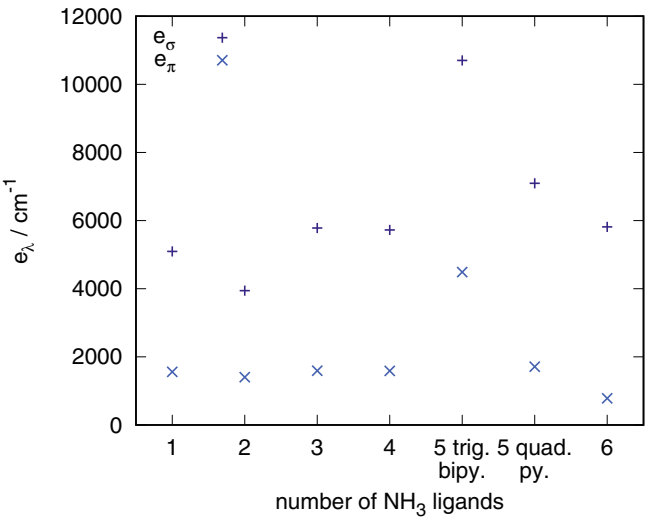

FIGURE 3 AOM parameters of ammonia in $[Mn(NH_3)_n]^{2+}$. The two $n = 5$ geometries are labeled.

The mutual dependence of e_σ and e_{ds} was noted recently by Deeth, who stated "[...] the extent of σ bonding is no longer directly linked to the size of e_σ but rather it is masked by the d–s mixing."[58] One might also say that without the d–s mixing parameter, the σ parameter of the ligand is artificially lowered since it then absorbs the effect of the admixture of the s orbital. In this case, the "true" σ interaction would be higher than reflected in the parameter value. Both interpretations work within the framework of the AOM, so it is difficult to decide on that basis which one is more appropriate.

The trigonal bipyramidal structure is an example where the parameterization with AOMadillo does not suffice to capture all effects. Its parameters have very high magnitudes, which are essentially unaffected by different grouping options and inclusion of d–s mixing. This complex appears to be an example where d–p mixing effects should not be omitted, as pointed out by Smith.[12] In the given

TABLE 3 AOM expressions for d orbital energies in a trigonal bipyramidal complex in different parameterizations.

Orbital	AOMadillo parameter set	Manually adapted parameter set
d_{z^2}	$2.75e_\sigma - 0.25e_{ds}$	$2.75e_\sigma$
d_{xz}	$3.5e_\pi$	$3.5e_\pi$
d_{yz}	$3.5e_\pi$	$3.5e_\pi$
d_{xy}	$1.125e_\sigma + 1.5e_\pi$	$1.125e_\sigma + 1.5e_\pi - C_{dp}$
$d_{x^2-y^2}$	$1.125e_\sigma + 1.5e_\pi$	$1.125e_\sigma + 1.5e_\pi - C_{dp}$

D_{3h} symmetry, the d_{xy} and $d_{x^2-y^2}$ orbitals are allowed to mix with the p_x and p_y orbitals. Additionally, d–s mixing is expected for the d_{z^2} orbital. The MO coefficients of the active space show that there is almost no d–s mixing with the d_{z^2} orbital (90.9% d_{z^2}, 0.1% *s*), but indeed a considerable p character in the $d_{xy}/d_{x^2-y^2}$ orbitals (94.4% $d_{xy}/d_{x^2-y^2}$, 1.7% p_y/p_x).[†] We tested a parameterization with slight changes: e_{ds} is set to 0, but we introduced a correction term C_{dp} that decreases the energy of the $d_{xy}/d_{x^2-y^2}$ orbitals. The equations we used are presented in Table 3. With this set of parameters in an ideal D_{3h} geometry, the equation system is underdetermined and at least one parameter needs to be fixed. Setting $e_\sigma = 5800\,\mathrm{cm}^{-1}$ as an example, we obtain $e_\pi = 631\,\mathrm{cm}^{-1}$ and $C_{dp} = 2319\,\mathrm{cm}^{-1}$. We emphasize that C_{dp} is a correction term which subsumes angular factors F_{dp} that would be present in a systematic way of treating d–p mixing. Thus it cannot be compared to other parameters.

Other structures show similar fractions of *p* orbital admixture, but d–p mixing is absorbed in other parameters. In the trigonal bipyramid, no other parameter can subsume the d–p mixing effect and it must be accounted for explicitly to achieve a reasonable fit. A similar effect explains the extraordinarily large d–s mixing parameter of the quadratic pyramid. Here, a significant d–p mixing contribution is subsumed in e_{ds}, rendering it surprisingly large.

We can conclude that the parameters of ammonia in the given geometries are relatively consistent amongst each other. However, the series shows that the overall symmetry of a complex must be kept in mind (as for $n = 2$ and $n = 5$) and that it is always possible to encounter geometries for which no reasonable fit can be obtained. Lastly, it is important to emphasize that AOM parameters are bond length dependent, a variable that substantially changes among different heteroleptic complexes. We caution to transfer parameters; this is conceivable only for similar bond lengths, or when using a scan of the respective metal-ligand distance to evaluate the effect on the respective e_λ parameters.

7.3 | $[PtA_2B_2]$

Cisplatin *cis*-$[PtCl_2(NH_3)_2]$ and its homoleptic analogues are well known complexes with planar geometries.[59,60] We investigated the homoleptic complexes of Pt^{2+} with chloride, ammonia and water as ligands as well as their heteroleptic $[PtA_2B_2]^{n+}$ counterparts. The results are shown in Table 4. It is apparent that the homoleptic complexes yield consistent and plausible parameters with d–s mixing included. The values for the ammonia ligands fit well to experimental values, while the chloride parameters seem to be underestimated.[59] Excluding d–s mixing leads to a very high cost, since the position of the d_{z^2} orbital cannot be accounted for. The heteroleptic complexes are much more complicated: While the π parameters of the *trans* complexes are stable with a small standard deviation, the parameters for the *cis* complexes appear random. The full results over all samples suggest that there is a dependency between e_σ and e_{ds}, whereas e_π is well defined with the given orbital splitting.

To visualize the dependency between e_σ and e_{ds}, we performed a scan along e_{ds} of the water ligands for a single sample of $[PtCl_2(H_2O)_2]$. The resulting parameters are shown in Figure 4. We can see that there is a cost minimum around $e_{ds} = 2300\,\mathrm{cm}^{-1}$, but it is very shallow. The second panel of Figure 4 illustrates the dependency of e_{ds} and e_σ, with an apparently linear relationship to e_σ of the water ligand. Not depicted but also part of the dependency is e_{ds} of the chloride ligands. In contrast, e_{ds} and e_π are essentially unrelated, as shown in the third panel. Performing the same scan for different samples yields slightly shifted, but qualitatively equal curves. The *trans* complexes are a good example of a partial underdetermination, where some of the orbital energies are well defined, while others are overparameterized.

As apparent in Table 4, the *cis* complexes do not yield a stable or plausible result. The reason is a splitting in the d_{xz} and d_{yz} orbitals that should be degenerate in the AOM parameterization with ligands A and B. Both orbital energies are expressed as

$$\varepsilon_{d_{xz}} = \varepsilon_{d_{yz}} = e_{\pi,A} + e_{\pi,B}, \tag{11}$$

but are found with a difference $\varepsilon_{d_{xz}} - \varepsilon_{d_{yz}} = 512\,\mathrm{cm}^{-1}$ in the aiLFT analysis.

Such an unexpected orbital energy splitting has been observed for other planar *cis* complexes. Hitchman noticed this type of splitting for Co(salen),[61] which was later attributed to the phase-coupling in the salen ligand.[35] Since the Pt complexes studied here do not have phase-coupled ligators, the cause of the d orbital splitting is unclear. Deeth attributed it to an asymmetric π-interaction of coordination voids on the z-axis.[26]

Without a specific parameter that accounts for the observed energy splitting, the fit cannot work well, making e_π indeterminable. Additionally, the dependency of e_σ and e_{ds} remains a problem as for the *trans* complexes, making it impossible to obtain a reasonable AOM parameterization.

7.4 | $[Cu(NH_3)_4(SCN)_2]$

$[Cu(NH_3)_4(SCN)_2]$ is a good example of a complex where different parameterizations work well. The geometry is taken from the crystal structure; the coordination units are separate and no other ions are

TABLE 4 AOM parameters of different planar $[PtA_4]^{n+}$ and $[PtA_2B_2]^{n+}$ complexes with the ligands chloride, ammonia and water.

Complex	e_σ/cm^{-1}	e_π/cm^{-1}	e_{ds}/cm^{-1}	e_σ/cm^{-1}	e_π/cm^{-1}	e_{ds}/cm^{-1}
	Cl			NH_3		
$[PtCl_4]^{2-}$	8739 (1)	1710 (1)	2297 (1)			
$[Pt(NH_3)_4]^{2+}$				14109 (5)	1670 (4)	2842 (2)
trans-$[PtCl_2(NH_3)_2]$	8770 (1873)	3097 (1)	1298 (933)	23939 (5896)	497 (5)	8525 (2950)
cis-$[PtCl_2(NH_3)_2]$	14380 (6382)	4364 (451)	5842 (3748)	9498 (6488)	−1244 (472)	2493 (3281)
	Cl			H_2O		
$[PtCl_4]^{2-}$	8739 (1)	1710 (1)	2297 (1)			
$[Pt(H_2O)_4]^{2+}$				13335 (71)	3946 (102)	1421 (15)
trans-$[PtCl_2(H_2O)_2]$	10496 (6684)	1811 (6)	3574 (3309)	13938 (6384)	652 (55)	3957 (3219)
cis-$[PtCl_2(H_2O)_2]$	10267 (1899)	1379 (1123)	160 (319)	9568 (1844)	1688 (1093)	9012 (1932)
	NH_3			H_2O		
$[Pt(NH_3)_4]^{2+}$	14109 (5)	1670 (4)	2842 (2)			
$[Pt(H_2O)_4]^{2+}$				13335 (71)	3946 (102)	1421 (15)
trans-$[Pt(NH_3)_2(H_2O)_2]^{2+}$	20168 (9369)	2525 (20)	6173 (4686)	18607 (9373)	2683 (18)	4259 (4684)
cis-$[Pt(NH_3)_2(H_2O)_2]^{2+}$	34348 (16,547)	21746 (12246)	3891 (3518)	−6821 (16588)	−16587 (12246)	3242 (3540)

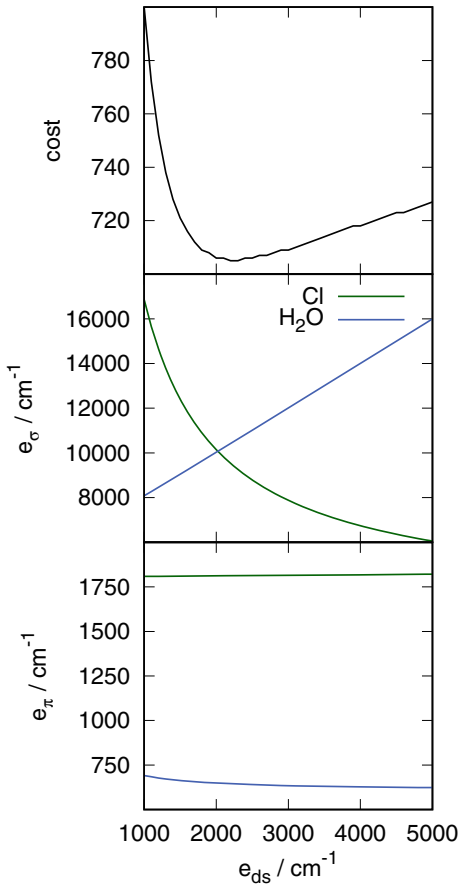

FIGURE 4 AOM parameters and cost of the fits for a single sample of *trans*-$[PtCl_2(H_2O)_2]$ while scanning along e_{ds} of the water ligands. Fits are obtained with each chloride and water in a group. Steps in the cost plot are caused by the integer resolution of the fit output.

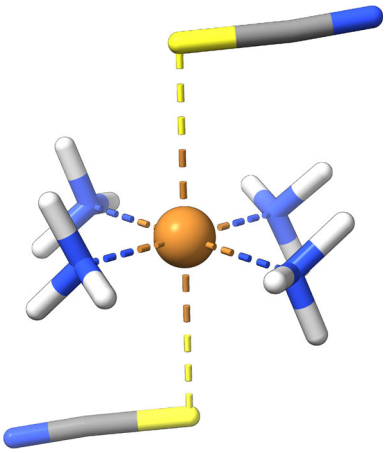

FIGURE 5 Coordination unit of $Cu(NH_3)_4(SCN)_2$. Notice the bent Cu–S=CN bond that suggests a distinction between π_x and π_y interactions and explains the pronounced misdirected valency.

present in the crystal.[47] Hydrogen atoms were added to complete the ammine ligands and a H-only geometry optimization was performed,[‡] see Figure 5 for the optimized structure. The sampling procedure was applied and different parameterizations were tested, shown in Table 5. It is interesting to note that the three parameterizations shown yield reasonable parameters, although at different costs. The remaining, relatively high costs in each fit can be explained by a significant misdirected valency because of the bent Cu–S=CN bond, which we cannot capture.

With a D_{4h} coordination sphere, one must in principle consider d–s mixing. However, Gerloch, Woolley, and Deeth showed that placing imaginary ligands at the z-axis can account for the low energy of

TABLE 5 Parameters for $Cu(NH_3)_4(SCN)_2$ with different parameterizations.

Ligand	Parameter/cm^{-1}	no d–s, one e_π	d–s, one e_π	d–s, two e_π
NH_3	e_σ	3604 (141)	3686 (79)	3769 (76)
	e_{π_x}	114 (108)	170 (59)	232 (59)
	e_{π_y}			232 (58)
	e_{ds}		567 (15)	564 (15)
SCN	e_σ	−779 (133)	356 (61)	438 (62)
	e_{π_x}	−495 (97)	−429 (54)	−400 (51)
	e_{π_y}			−330 (57)
	e_{ds}		1 (1)	0 (1)
Cost		71065 (7441)	6227 (1281)	4507 (1067)

Note: All AOM parameters in /cm^{-1}.

TABLE 6 AOM parameters for a series of $[Fe(H_2O)_{6-n}(NCS)_n]^{(3-n)+}$ complexes with different configurations.

Complex	H_2O		H_2O'		NCS^-	
	e_σ/cm^{-1}	e_π/cm^{-1}	e_σ/cm^{-1}	e_π/cm^{-1}	e_σ/cm^{-1}	e_π/cm^{-1}
m6 $[Fe(H_2O)_6]^{3+}$	4527 (205)	1055 (154)				
m6 $[Fe(H_2O)_5(NCS)]^{2+}$	3321 (150)	694 (81)			9997 (99)	4823 (63)
m4 $[Fe(H_2O)_5(NCS)]^{2+}$	6500 (24)	974 (21)	1397 (11)	412 (7)	11236 (10)	6493 (11)
m6 *trans*-[Fe(H2O)4(NCS)2]+ [a]	2553 (284)	311 (215)			7715 (282)	2405 (212)
m4 *trans*-$[Fe(H_2O)_4(NCS)_2]^+$ [b]	6309 (14)	1255 (8)	1225 (14)	598 (5)	10,488 (8)	4130 (12)
m6 *cis*-$[Fe(H_2O)_4(NCS)_2]^+$	1877 (150)	−49 (77)			8172 (51)	2544 (34)
m4 *cis*-$[Fe(H_2O)_4(NCS)_2]^+$ [b]	4573 (929)	3511 (686)	15300 (1753)	7962 (1397)	6360 (642)	331 (531)
m2 *cis*-$[Fe(H_2O)_4(NCS)_2]^+$ [b]	2479 (225)	−1342 (154)	1412 (244)	−586 (176)	8316 (265)	415 (195)
m2 *cis*-$[Fe(H_2O)_4(NCS)_2]^+$ [b]	2274 (356)	−1099 (384)			7770 (194)	762 (182)
m6 trig.-bipy. $[Fe(H_2O)_2(NCS)_3]$ [c]	388 (106)	−256 (127)			6269 (232)	−1160 (81)
m4 *mer*-$[Fe(H_2O)_3(NCS)_3]$ [b]	8067 (1434)	5109 (958)			15583 (1366)	6855 (903)
m6 $[Fe(H_2O)_2(NCS)_3]$ [c]	1386 (153)	90 (102)			6312 (663)	1179 (347)
m4 *fac*-$[Fe(H_2O)_3(NCS)_3]$ [b]	4505 (906)	1839 (352)			9778 (804)	3032 (265)

Note: For water sometimes two parameter sets are given in case of different M–O bond lengths.
[a]Interestingly, the inclusion of d–s mixing does not change the fit substantially.
[b]Not the ground state multiplicity.
[c]Five-coordinate.

the d_{z^2} orbital as well. These coordination voids then have a negative e_σ and an e_π of 0.[4,13,62,63] Indeed, the fits show that the SCN^- ligands, lying on the z-axis, subsume the effect of d–s mixing in their σ parameter. When fitting without d–s mixing parameter, SCN^- seems to be a σ acceptor. With d–s mixing considered, it changes from an acceptor to a weak donor. Of course it is not the chemistry that changes, but rather its projection onto the model. Assuming that SCN^- being a σ acceptor is unlikely, this example shows that the concept of the coordination void (besides other disadvantages that have been noted in the literature[33]) might not adequately reproduce the ligand field splitting of these MA_4B_2 quasi D_{4h} complexes. Including a separation of π_x and π_y interactions to account for the bent Cu–S=CN bond does not generally alter the picture. The splitting of the π parameters is small and does not justify an interpretation.

In this example, three different parameterizations yield plausible results and one has to check carefully which one is the most useful, that is, which one can be interpreted chemically. In this case, the first parameterization without e_{ds} leads to a negative e_σ, which seems improbable. The second and third one yield similar results with a much lower cost than the first fit. Since overparameterization is an omnipresent danger when dealing with the AOM, we would prefer the second set with subsumed e_π parameters.

7.5 | Ferric thiocyanates

The heteroleptic $[Fe(H_2O)_{6-n}(NCS)_n]^{(3-n)+}$ complexes are known for their intense red color and serve as a qualitative tool for the detection

of Fe^{3+} ions.[64] Although the characteristic color emerges from a charge-transfer instead of a d-d transition, the stability and variety of this family of complexes makes it a good example for the same ligand having strongly varying parameters in different bonding situations. The thiocyanate ion can coordinate via the sulfur or nitrogen atom. Based on the HSAB principle,[65] the hard Fe^{3+} ion is likely to prefer a hard Lewis base, hence the Fe–NCS coordination is to be expected. This is supported by experimental evidence[66] as well as our calculations, which predict the nitrogen coordinating complexes to be ca. 60 kJ/mol^{-1} more stable than the sulfur coordinating ones in the $n = 1$ case. We investigated and present complexes with $n = 0 - 3$, which includes the *cis* and *trans* configurations for $n = 2$ and the *fac* and *mer* configurations for $n = 3$. The high-spin $n = 3$ complexes are not stable in our solvent-free calculations, they lose one water ligand and form 5-coordinate complexes.

The obtained data is presented in Table 6. It is apparent that the range of parameter values is very large. They differ among the complexes and depend largely on bond distance, global symmetry and other ligands. Here, these dependencies are intertwined in a way that it is impossible to separate them. Transferability issues are well known[7] and especially the mutual influence of *trans* ligands was discussed critically.[8] This again shows that transferability of AOM parameters between complexes is extremely limited, even between stereoisomers.

8 | CONCLUSIONS

With the above examples and the ones in previous publications[21,25] it is shown that our procedure can be applied to a variety of transition metal complexes. Nonetheless, the user must be careful and aware of problems and ambiguities in the AOM parameterization choices that might not be obvious.

In the example of $[Cu(NH_3)_4(SCN)_2]$, we saw that different parameterizations for the same complex may work well and yield equally reasonable parameter sets. It is not obvious at first glance which parameterization is the one that corresponds best to the chemistry of the complex. We suggest to refer to the expected properties of the ligands in order to rule out certain results.

The example of ligand addition from a metal-ligand pair up to an octahedral complex brought up a similar problem and another way of treating it: while knowing that the linear $[Mn(NH_3)_2]^{2+}$ should have a d–s mixing contribution, its magnitude cannot be determined from the single complex itself. Comparing the obtained AOM parameters with similar complexes gives us a hint of what the parameter is likely to be.

The last example of the ferric thiocyanates brings us close to the boundaries of both approaches. Due to the effects that different ligands have on each other, especially regarding their varying bond lengths in different complexes, the transfer of AOM parameters from one complex to another is delicate.[7–9] With the presented data set, it is difficult to determine with high confidence which set is reliable. Ideally, one would compare the obtained parameterization for such cases with experimental data from electronic absorption measurements or magnetic data.

In treating the platinum complexes, we showed that even for seemingly simple complexes, one can face difficulties to fit a reasonable set of AOM parameters. We showed an example of partial dependencies in the AOM equation system and cases where the parameterization does not fully work.

While the examples above were chosen to highlight challenges and pitfalls in applying the AOM to transition metal complexes, the utility of having an unbiased fitting tool was also demonstrated herein and in earlier works. The easy applicability of AOMadillo combined with the chemically intuitive AOM parameters make it a tool that might be used in teaching as well. With aiLFT results from ORCA, the transitions themselves can be discussed. When using AOMadillo to obtain AOM parameters, the students would be tasked with important choices regarding ligand grouping and parameter sets, while the mathematics are hidden. It is thus a good tool to test different parameterizations and study LFT and the AOM in a hands-on fashion.

There are many examples for which the combination of LFT, AOM and computational chemistry work in a clear and unambiguous way. As we showed in previous publications,[21,25] it is possible to perform bond length and angle scans that can be automatically parameterized by AOMadillo. Series over different transition metals or different formal oxidation states are often instructive: they yield results that can be parameterized well by the AOM and generally have clear interpretations. Sometimes trickier, but nevertheless often successful, are series with different ligands, where qualitative comparisons between ligands in similar environments can be made.

ACKNOWLEDGMENT

This work was funded by the Deutsche Forschungsgemeinschaft (DFG, German Research Foundation) – CRC 1487, “Iron, upgraded!” – project number 443703006. Open Access funding enabled and organized by Projekt DEAL.

DATA AVAILABILITY STATEMENT

Data from the case studies is available from the authors upon request. The program presented herein is freely available for academic research under https://git.rwth-aachen.de/ak-krewald/aomadillo.

ORCID

Moritz Buchhorn https://orcid.org/0000-0002-6800-1785
Vera Krewald https://orcid.org/0000-0002-4749-4357

ENDNOTES

* We note that distortions along normal modes are successfully employed in other research areas such as theoretical photochemistry or concepts for electron transfer; applying a Wigner-type sampling procedure here did not result in useful sample sets.

† For comparison, we found 1.3% *s* character in the d_{z^2} orbital of D_{4h} $[Cu(NH_3)_4]^{2+}$, which can be considered an archetypal example of d–s mixing.[25]

‡ If optimized freely, the SCN^- ligands orient themselves to the hydrogen atoms and a Cu–SCN–H–N–Cu pseudo-cycle forms.

REFERENCES

[1] C. E. Schäffer, C. K. Jørgensen, *Mol. Phys.* **1965**, *9*, 401.
[2] B. N. Figgis, M. A. Hitchman, *Ligand Field Theory and Its Applications*, 1st ed., Wiley-VCH, New York **2000**.
[3] M. Gerloch, R. G. Woolley, in *Progress in Inorganic Chemistry* (Ed: S. J. Lippard), John Wiley & Sons, Interscience, New York **1984**, p. 371.
[4] M. Gerloch, J. H. Harding, R. G. Woolley, *Inorganic Chemistry*, Springer, Berlin **1981**, p. 1.
[5] I. Bertini, D. Gatteschi, A. Scozzafava, *Inorg. Chem.* **1975**, *14*, 812.
[6] T. Schönherr, in *Topics in current chemistry* (Ed: H. Yersin), Springer, Berlin **1997**, p. 87.
[7] M. Gerloch, R. G. Woolley, *J. Chem. Soc., Dalton Trans.* **1981**, 1714.
[8] D. W. Smith, *Inorg. Chem.* **1978**, *17*, 3153.
[9] A. J. Bridgeman, M. Gerloch, in *Progress in Inorganic Chemistry* (Ed: K. D. Karlin), Wiley, New York **1996**, p. 179.
[10] M. Atanasov, D. Ganyushin, K. Sivalingam, F. Neese, in *Molecular Electronic Structures of Transition Metal Complexes II*. Structure and Bonding (Ed: D. M. P. Mingos), Springer, Berlin **2011**, p. 149.
[11] M. Suta, F. Cimpoesu, W. Urland, *Coord. Chem. Rev.* **2021**, *441*, 213981.
[12] D. W. Smith, *Inorg. Chim. Acta* **1977**, *22*, 107.
[13] R. J. Deeth, D. L. Foulis, *Phys. Chem. Chem. Phys.* **2002**, *4*, 4292.
[14] F. Neese, *Wiley Interdiscip. Rev.: Comput. Mol. Sci.* **2012**, *2*, 73.
[15] F. Neese, *Wiley Interdiscip. Rev.: Comput. Mol. Sci.* **2018**, *8*, e1327.
[16] E. A. Suturina, D. Maganas, E. Bill, M. Atanasov, F. Neese, *Inorg. Chem.* **2015**, *54*, 9948.
[17] D. Schweinfurth, M. G. Sommer, M. Atanasov, S. Demeshko, S. Hohloch, F. Meyer, F. Neese, B. Sarkar, *J. Am. Chem. Soc.* **2015**, *137*, 1993.
[18] S. K. Singh, J. Eng, M. Atanasov, F. Neese, *Coord. Chem. Rev.* **2017**, *344*, 2.
[19] V. G. Chilkuri, S. DeBeer, F. Neese, *Inorg. Chem.* **2017**, *56*, 10418.
[20] V. G. Chilkuri, S. DeBeer, F. Neese, *Inorg. Chem.* **2020**, *59*, 984.
[21] M. Buchhorn, R. J. Deeth, V. Krewald, *Chem. – Eur. J.* **2022**, *28*, e202103775.
[22] W. H. Press, *Numerical Recipes: The Art of Scientific Computing/William H. Press … [et al.]*, 3rd ed., Cambridge University Press, Cambridge **2007**.
[23] P. Virtanen, R. Gommers, T. E. Oliphant, M. Haberland, T. Reddy, D. Cournapeau, E. Burovski, P. Peterson, W. Weckesser, J. Bright, S. J. van der Walt, M. Brett, J. Wilson, K. J. Millman, N. Mayorov, A. R. J. Nelson, E. Jones, R. Kern, E. Larson, C. J. Carey, İ. Polat, Y. Feng, E. W. Moore, J. VanderPlas, D. Laxalde, J. Perktold, R. Cimrman, I. Henriksen, E. A. Quintero, C. R. Harris, A. M. Archibald, A. H. Ribeiro, F. Pedregosa, P. van Mulbregt, *Nat. Methods* **2020**, *17*, 352.
[24] P. Virtanen, R. Gommers, T. E. Oliphant, M. Haberland, T. Reddy, D. Cournapeau, E. Burovski, P. Peterson, W. Weckesser, J. Bright, S. J. van der Walt, M. Brett, J. Wilson, K. J. Millman, N. Mayorov, A. R. J. Nelson, E. Jones, R. Kern, E. Larson, C. J. Carey, İ. Polat, Y. Feng, E. W. Moore, J. VanderPlas, D. Laxalde, J. Perktold, R. Cimrman, I. Henriksen, E. A. Quintero, C. R. Harris, A. M. Archibald, A. H. Ribeiro, F. Pedregosa, P. van Mulbregt, *Nat. Methods* **2020**, *17*, 261.
[25] M. Buchhorn, V. Krewald, *Dalton Trans.* **2023**, *52*, 6685.
[26] R. J. Deeth, *Eur. J. Inorg. Chem.* **2020**, *2020*, 1960.
[27] D. W. Clack, C. Mingdan, K. D. Warren, *J. Mol. Struct.: THEOCHEM* **1987**, *153*, 323.
[28] A. Trueba, P. Garcia-Fernandez, J. M. Garcia-Lastra, J. A. Aramburu, M. T. Barriuso, M. Moreno, *J. Phys. Chem. A* **2011**, *115*, 1423.
[29] F. Neese, L. Lang, V. G. Chilkuri, in *Topology, Entanglement, and Strong Correlations* (Eds: E. Pavarini, E. Koch), Forschungszentrum Jülich, Jülich **2020**.
[30] M. Atanasov, P. Comba, C. A. Daul, F. Neese, in *Models, Mysteries, and Magic of Molecules* (Eds: J. C. A. Boeyens, J. F. Ogilvie), Springer, Dordrecht, The Netherlands **2008**, p. 411.
[31] F. Neese, F. Wennmohs, *ORCA 4.2.1 Manual*, Max-Planck-Institut für Kohleforschung, Mülheim an der Ruhr **2019**.
[32] F. Neese, F. Wennmohs, *ORCA 5.0.4 Manual*, Max-Planck-Institut für Kohleforschung, Mülheim an der Ruhr **2021**.
[33] C. E. Schäffer, *Inorg. Chim. Acta* **1995**, *240*, 581.
[34] A. Ceulemans, M. Dendooven, L. G. Vanquickenborne, *Inorg. Chem.* **1985**, *24*, 1153.
[35] A. Ceulemans, M. Dendooven, L. G. Vanquickenborne, *Inorg. Chem.* **1985**, *24*, 1159.
[36] C. E. Schäffer, H. Yamatera, *Inorg. Chem.* **1991**, *30*, 2840.
[37] M. A. Atanasov, T. Schönherr, H.-H. Schmidtke, *Theor. Chim. Acta* **1987**, *71*, 59.
[38] T. Schönherr, M. Atanasov, H. Adamsky, in *Comprehensive Coordination Chemistry II* (Eds: J. A. McCleverty, T. J. Meyer), Elsevier Pergamon, London **2004**, p. 443.
[39] R. J. Deeth, M. J. Duer, M. Gerloch, *Inorg. Chem.* **1987**, *26*, 2573.
[40] R. J. Deeth, M. J. Duer, M. Gerloch, *Inorg. Chem.* **1987**, *26*, 2578.
[41] R. J. Deeth, M. Gerloch, *Inorg. Chem.* **1987**, *26*, 2582.
[42] M. J. Duer, N. D. Fenton, M. Gerloch, *Int. Rev. Phys. Chem.* **1990**, *9*, 227.
[43] A. Bronova, T. Bredow, R. Glaum, W. Urland, *Inorg. Chem.* **2016**, *55*, 6853.
[44] J. Jung, M. Atanasov, F. Neese, *Inorg. Chem.* **2017**, *56*, 8802.
[45] W. Urland, *Chem. Phys.* **1976**, *14*, 393.
[46] M. A. Morrison, G. A. Parker, *Aust. J. Phys.* **1987**, *40*, 465.
[47] M. A. Porai-Koshits, *J. Struct. Chem.* **1964**, *4*, 531.
[48] A. D. Becke, *Phys. Rev. A* **1988**, *38*, 3098.
[49] J. P. Perdew, *Phys. Rev. B* **1986**, *33*, 8822.
[50] F. Weigend, R. Ahlrichs, *Phys. Chem. Chem. Phys.* **2005**, *7*, 3297.
[51] F. Weigend, *Phys. Chem. Chem. Phys.* **2006**, *8*, 1057.
[52] E. J. Baerends, D. E. Ellis, P. Ros, *Chem. Phys.* **1973**, *2*, 41.
[53] O. Vahtras, J. Almlöf, M. W. Feyereisen, *Chem. Phys. Lett.* **1993**, *213*, 514.
[54] P. Siegbahn, A. Heiberg, B. Roos, B. Levy, *Phys. Scr.* **1980**, *21*, 323.
[55] B. O. Roos, P. R. Taylor, P. E. Siegbahn, *Chem. Phys.* **1980**, *48*, 157.
[56] C. van Wüllen, *J. Chem. Phys.* **1998**, *109*, 392.
[57] D. A. Pantazis, F. Neese, *WIREs Comput. Mol. Sci.* **2014**, *4*, 363.
[58] R. J. Deeth, *Eur. J. Inorg. Chem.* **2022**, *2022*, e202100936.
[59] L. G. Vanquickenborne, A. Ceulemans, *Inorg. Chem.* **1981**, *20*, 796.
[60] A. J. Bridgeman, M. Gerloch, *J. Chem. Soc., Dalton Trans.* **1995**, 197.
[61] M. A. Hitchman, *Inorg. Chem.* **1977**, *16*, 1985.
[62] R. J. Deeth, M. Gerloch, *Inorg. Chem.* **1984**, *23*, 3846.
[63] R. G. Woolley, *Int. Rev. Phys. Chem.* **1987**, *6*, 93.
[64] S. A. Lewin, R. S. Wagner, *J. Chem. Educ.* **1953**, *30*, 445.
[65] R. G. Pearson, *J. Am. Chem. Soc.* **1963**, *85*, 3533.
[66] T. J. Conocchioli, N. Sutin, *J. Am. Chem. Soc.* **1967**, *89*, 282.

How to cite this article: M. Buchhorn, V. Krewald, *J. Comput. Chem.* **2024**, *45*(2), 122. https://doi.org/10.1002/jcc.27224